Preprints, 10th IFAC International Symposium on
Advances in Automotive Control
Columbus, Ohio, USA, August 28-30, 2022

Model Predictive Control of Combustion Phasing in Compression Ignition Engines by Coordinating Fuel Injection Timing and Ignition Assist

Omar Y. Ahmed * **Robert J. Middleton** * **Vivian Tran** *
Andrew Weng * **Anna G. Stefanopoulou** * **Kenneth S. Kim** **
Chol-Bum M. Kweon **

* *Department of Mechanical Engineering, University of Michigan - Ann Arbor, Ann Arbor, MI 48109*
** *U.S. Army Combat Capabilities Development Command Army Research Laboratory, Aberdeen Proving Ground, MD 21005*

Abstract: Internal combustion engines may use ignition assisting heating elements such as glow plugs to facilitate combustion control in automotive or aircraft powertrains that operate with synthetic fuels of varying ignition behavior or at extreme inlet conditions. This work presents a model predictive controller (MPC) that regulates combustion phasing in compression ignition engines on a cycle-to-cycle basis by coordinating fuel start of injection (SOI) with power supplied to a glow plug acting as an ignition assist (IA) device, while enforcing IA actuator range and rate constraints. Simulations were conducted using a nonlinear virtual engine informed by data from a commercial engine operating at a condition that induced high combustion variability. A rate-based MPC formulation leveraging state estimate feedback and integral setpoint tracking was developed. Simulation results show the MPC scheme ensures steady-state tracking of combustion phasing within 70 engine cycles, conserves IA usage whenever possible to reduce thermo-mechanical stress on the actuator, and maintains closed-loop combustion variability at only 4% higher than the open-loop system variability. Furthermore, the controller maintains reference tracking even if combustion sensitivity to the actuators deviates by more than 20% from the controller's internal model, without the need for retuning control parameters.

Keywords: Model predictive control, internal combustion engine control, ignition assist

1. INTRODUCTION

To improve sustainability and reduce environmental impact in the automotive and aviation sectors, synthetic and low-carbon fuels are becoming increasingly prevalent for use in internal combustion engines that use compression ignition (CI). Biodiesel, produced via transesterification of bio-oils, has been researched for ground vehicles because its combustion behavior is very similar to that of petroleum-based fuels (Agarwal, 2007). Biodiesel has also been studied for aircraft engines, along with hydroprocessed renewable jet fuels and Fischer-Tropsch fuels produced by catalytic conversion of biomass-generated syngas (Yilmaz and Atmanli, 2017). However, these fuels have subpar properties for the low pressure and temperature conditions of aviation (Yilmaz and Atmanli, 2017). Improvements in combustion control strategies for CI engines may help overcome these barriers and support a wider range of alternative fuel options, even if they have more varied ignition behavior.

Traditional CI combustion control comprises feedforward maps that dictate fuel injection quantity and timing to meet a desired combustion phasing (Hillion et al., 2009). Phasing refers to when combustion occurs during an engine cycle to generate torque (Hillion et al., 2009). Feedforward maps are calibrated to a finite range of inlet conditions and fuel blends, and thus suffer against varying or uncertain fuel quality (Hillion et al., 2009).

Closed-loop combustion control employs cycle-to-cycle feedback, often from an in-cylinder pressure transducer, to characterize combustion phasing in real-time and adjust fuel injection and other actuators to maintain desired combustion behavior (Willems, 2018). One form of feedback control is model predictive control (MPC), which can account for constraints on actuators or system states. MPC schemes have been investigated in engine control to coordinate actuators such as EGR, VGT, and injection timing for emissions reduction and torque regulation (Duraiarasan et al., 2021; Bergmann et al., 2021). Closed-loop control strategies can reduce the impact of poor fuel quality and non-ideal ambient conditions, but challenges remain in efficiently coordinating multiple actuators and in managing the inherent cycle-to-cycle variability (CV) of the stochastic combustion process (Willems, 2018).

Most commercial CI engines are equipped with glow plugs, which are resistive heating elements that reside in-cylinder and transfer thermal energy to air-fuel mixtures to facilitate combustion. Glow plugs commonly activate for a lim-

ited duration to assist cold start in accordance with open-loop calibrations (Zhou et al., 2016). Recently, they have been researched as continuously active ignition assist (IA) devices to enable combustion and shift phasing (Ahmed et al., 2021b; Lawler et al., 2018). Figure 1 plots engine data showing how glow plugs can shift in-cylinder pressure, advance combustion phasing, and reduce CV.

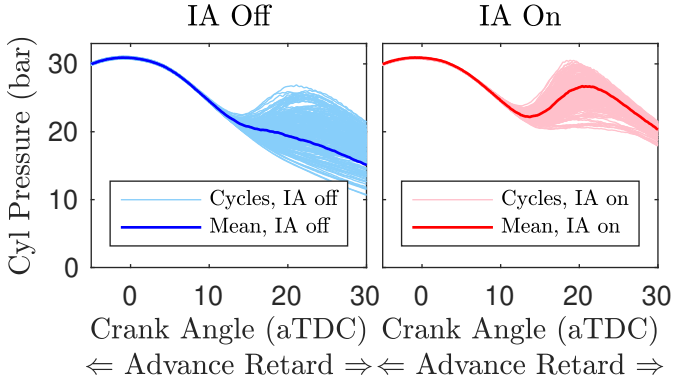

Fig. 1. An ignition assist (IA) device advances combustion phasing and reduces cycle-to-cycle variability.

Glow plugs may be used as secondary IA actuators that augment the control authority of fuel injection timing when needed to regulate combustion phasing. However, at certain speeds and loads, current commercial devices need to be powered higher than their rated voltage to reach sufficient surface temperature in-cylinder, due to the convective cooling effect of inducting air charges (Motily et al., 2021). This overdriving may degrade the resistive heating element in the long term. Ceramic IA devices have superior temperature capability, but are brittle and may physically fragment if thermally overloaded during aggressive transient actuation (Oprea et al., 2012). IA actuators are prone to a combination of chemical, mechanical, thermal, and electrical failure mechanisms, motivating careful feedback control that enforces certain power rate and range constraints (Oprea et al., 2012).

We first investigated feedback combustion control using IA in our previous work (Ahmed et al., 2021a). Here, a PI loop informed fuel start of injection (SOI) as the primary actuator on a cycle-to-cycle basis for fast response, and conditionally activated IA to full power when SOI reached its range limit. This approach for actuator coordination ensured sufficient control authority, but it simply toggled the IA between its "off" and "full power" states as needed. Accounting for more advanced IA actuation constraints would require additional development.

An MPC approach may better incorporate IA constraints during real-time control. The authors are aware of no existing studies that have applied MPC schemes to thermal IA devices for engines. Thus, this work presents an investigation of a model predictive control architecture that coordinates fuel start of injection with ignition assist to control combustion phasing while enforcing IA actuator rate and range constraints.

2. COMBUSTION PHASING MODEL

In previous work, engine experiments informed a nonlinear virtual engine to simulate combustion phasing mean and dispersion (Ahmed et al., 2021b). Those efforts are summarized here, then used to derive a linear state-space representation of the system to facilitate MPC design. Actuator range and rate constraints are also presented.

2.1 Data-Driven Nonlinear Virtual Engine

Experiments were conducted in a Ford 6.7 L Powerstroke commercial CI engine mated to a dynamometer. Each of the engine's eight cylinders is equipped with a piezoelectric fuel injector, a stock metal glow plug for cold start assistance, and an in-cylinder pressure transducer. Experiments were conducted at 1200 rpm and approximately 2 bar BMEP using a fixed fueling strategy with pump-grade diesel (cetane 46-48). Coolant and inlet air temperatures were regulated to 15°C and 20°C, respectively. Intake manifold pressure was throttled down to 0.75 bar. These conditions thermodynamically emulate inlet conditions of interest for aviation, and qualitatively emulate high CV conditions induced by poorly igniting alternative fuels.

System characterization experiments comprised sweeps of SOI and step changes in IA power, both of which were repeated as the engine warmed up from cold start. The top row of Fig. 2 plots four combustion phasing step responses to IA activation at different SOI and increasingly warm engine thermal states, as indicated by the 50°C increase in exhaust gas temperature over the course of the test. The IA was activated to 57 W in alignment with the engine's open-loop map for glow plug actuation. As it heated up, the IA transferred thermal energy to the air-fuel mixture to shorten ignition delay, advance phasing, and reduce CV.

Experiments were used to regress a low-order nonlinear model for steady-state combustion phasing mean μ_{phas} (Eq. 1) and standard deviation σ_{phas} (Eq. 2). A quadratic functional form was employed for Eq. 1 to capture the nonlinear sensitivity of combustion phasing to SOI at late injection conditions. An exponential functional form was employed for Eq. 2 because CV in phasing was observed to increase steeply with ignition delay, defined as the delay between SOI and mean-value phasing ($\mu_{\text{phas}} - u_{\text{SOI}}$). The two actuator inputs u_{SOI} and u_{IA} are augmented with a third input for exhaust gas temperature T_{exh}. This parameter captures the engine's evolving thermal state and consequent effects on phasing and actuator control authority. Parameters u_0 and T_0 are fixed reference values for SOI and exhaust temperature, respectively. Coefficients α, β, γ, a, b, and c capture the coupling between inputs and outputs. Parameters were tuned to minimize the root mean square error between model output and experimental data.

$$\mu_{\text{phas}} = \alpha(u_{\text{SOI}} - u_0)^2 - \beta(T_{\text{exh}} - T_0) - \frac{\gamma}{(T_{\text{exh}} - T_0)} u_{\text{IA}} \tag{1}$$

$$\sigma_{\text{phas}} = \exp(a(\mu_{\text{phas}} - u_{\text{SOI}}) - b) + c \tag{2}$$

Figure 3 shows a block diagram of the virtual engine constructed for simulation. The two actuator inputs feed into transfer functions that capture their respective combustion response dynamics. Phasing responded to both actuators without any overshoot or oscillation, so 1$^{\text{st}}$-order transfer functions were deemed appropriate for both. Phasing exhibited an approximately 1-cycle response time to SOI

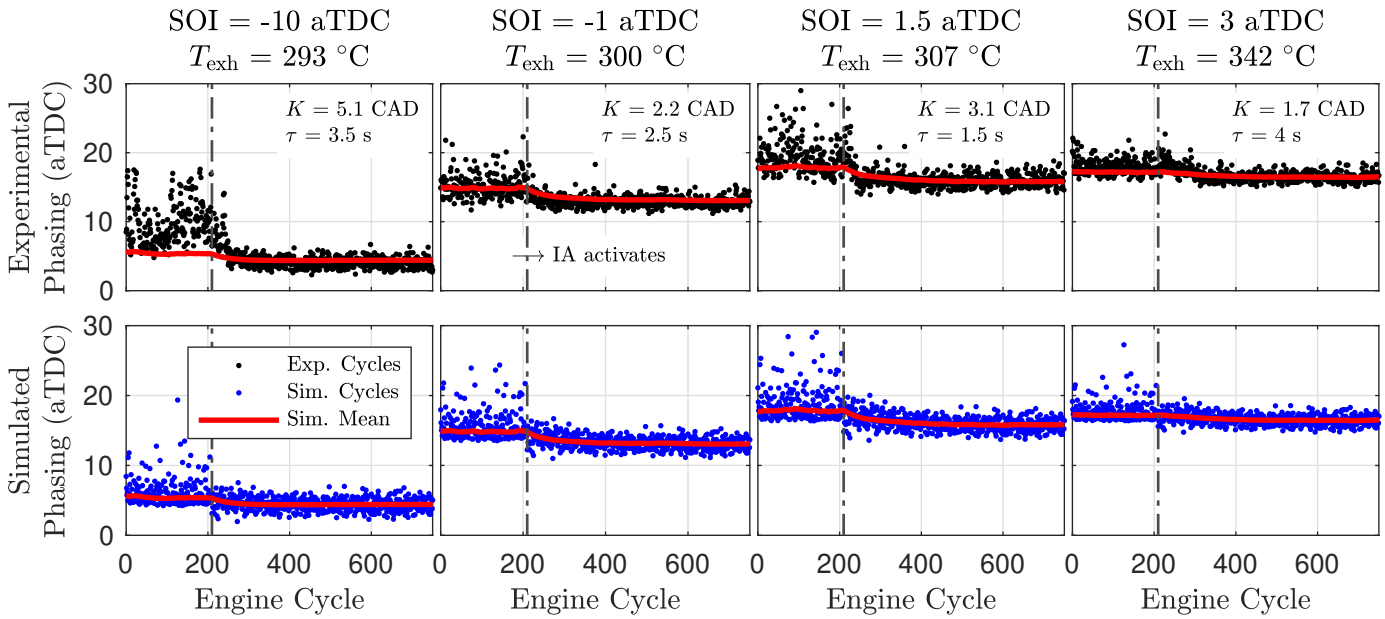

Fig. 2. Experimental (top) vs simulated (bottom) combustion phasing response to a step activation in IA at cycle 220 over the course of an engine warm-up experiment. The gain K and time constant τ of each step response is given.

actuation ($\tau_{\text{SOI}} = 0.1$ s at 1200 rpm). Phasing response to IA was an order of magnitude longer, due to the thermal inertia of the IA itself and heat transfer dynamics in the cylinder. Furthermore, data showed that phasing dynamics differed nontrivially if the IA turned on versus off. Therefore, two time constants are used: $\tau_{\text{IA,on}} = 3$ s and $\tau_{\text{IA,off}} = 6$ s.

The inputs then feed into the steady-state regressions given by Eq. 1 and 2. A stochastic noise sequence that scales according to the σ_{phas} regression simulates CV in the final phasing output. The bottom row of Fig. 2 plots the virtual engine's replications of the four step response experiments shown in the top row. The first 220 cycles of the leftmost simulation are erroneous because that condition was thermodynamically at the extreme edge of the tuning data range. Overall, the virtual engine accurately simulates phasing behavior as a function of SOI, IA, and engine thermal state.

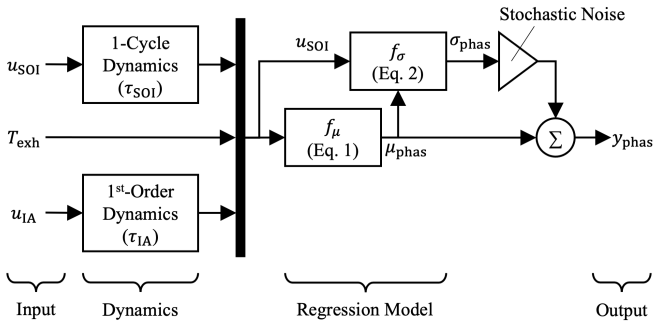

Fig. 3. Nonlinear virtual engine for simulation.

2.2 Linear State-Space Representation

To facilitate MPC design, a linear state-space version of the model from Section 2.1 was derived. Equation 3 shows a 2-input, 2-state model of system dynamics. Each state is a construct that captures the 1st-order combustion dynamics induced by its corresponding actuator, via the discrete-time equivalents of the time constants $\tau_{\text{SOI}} = 0.1$ s and $\tau_{\text{IA}} = 3$ s. Note that only the IA time constant for turning on was used here. Because Eq. 3 has unit DC gain, the states converge to the actuator inputs at steady-state.

Equation 4 then captures the steady-state linear gains in mean-value phasing as a function of actuator inputs. The average linear shifts in phasing per 1 crank angle degree (CAD) change in SOI and 1 W change in IA power were calculated using the step response data taken over the course of the warm-up experiments. These average shifts constituted the gain values in C. The linear system given in Eq. 3 and 4 is both controllable and observable using standard rank condition tests.

$$\underbrace{\begin{bmatrix} x_{\text{SOI}} \\ x_{\text{IA}} \end{bmatrix}_{k+1}}_{x_{k+1}} = \underbrace{\begin{bmatrix} 0.3679 & 0 \\ 0 & 0.9672 \end{bmatrix}}_{A} \underbrace{\begin{bmatrix} x_{\text{SOI}} \\ x_{\text{IA}} \end{bmatrix}_{k}}_{x_k} + \underbrace{\begin{bmatrix} 0.6321 & 0 \\ 0 & 0.03278 \end{bmatrix}}_{B} \underbrace{\begin{bmatrix} u_{\text{SOI}} \\ u_{\text{IA}} \end{bmatrix}_{k}}_{u_k} \tag{3}$$

$$y_{\text{phas},k} = \underbrace{[1.7 \;\; 0.03684]}_{C} x_k \tag{4}$$

It is worth recalling that steady-state gains in phasing are not always linear. For instance, the coupling between SOI and phasing is approximately linear at stable operating conditions, but becomes nonlinear as SOI retards and combustion behavior destabilizes. Such nuances were neglected when developing the linear state-space formulation for the controller because the ultimate goal of this work was to design an MPC scheme that guarantees reference phasing tracking even when its internal model does not perfectly match true combustion behavior.

2.3 Actuator Constraints

Actuator constraints used for simulations are listed in Table 1. In practice, SOI would have an advance limit to prevent excessively early ignition and destructively high peak pressures in-cylinder. The experiments informing the system model were conducted at very late injection timings to induce highly variable combustion, so a physically realistic advance limit was not relevant. Instead, for this work, an advance limit was chosen such that a reference tracking trajectory could be simulated in which both SOI and IA are needed. A maximum IA power in accordance with the 12 V rating for a commercial metal glow plug was enforced. An IA power ramp rate was chosen based on experimental procedures for actuating ceramic glow plugs. Such constraints would minimize IA device degradation and fragmentation due to thermo-mechanical stress.

Table 1. Actuator constraints for simulation.

Constraint	Min	Max
SOI	-9 aTDC Advance Limit	N/A
IA Power	0 W	80 W
IA Rate	N/A	2 W/cycle

3. CONTROLLER DESIGN

An ideal combustion phasing controller would ensure steady-state combustion phasing tracking, coordinate SOI and IA for rapid transient actuation, and enforce SOI and IA actuator constraints. This section details the use of a model-based estimator for state feedback and a rate-based integral reference tracking MPC formulation.

3.1 Model-Based Estimator

Cycle-to-cycle combustion phasing measurements capture the inherent physical variability in combustion behavior. This stochasticity can propagate and amplify through a feedback loop if not carefully managed. Thus, to reduce closed-loop CV, a Kalman filter acting as a model-based estimator was added:

$$\hat{x}_{k+1} = (A - LC)\hat{x}_k + Bu_k + Ly_{\text{phas},k} \tag{5}$$

$$\hat{y}_k = C\hat{x}_k. \tag{6}$$

Gain L is the solution of the steady-state Linear Quadratic Estimator (LQE) problem. Because true combustion process variation occurs in-cylinder and cannot be directly measured, it is assumed that measured combustion data encompasses both process noise and any sensor measurement noise to be rejected by the estimator. When solving the LQE for this work, process noise and measurement noise variance parameters were set to the lowest and highest experimentally observed phasing variances σ^2_{phas}, or 0.1 CAD and 4.4 CAD, respectively.

This model-based estimator rejects noise from the measurements and passes a smooth signal comprising state and phasing estimates to the controller. Because it uses the linear system model presented in Section 2.2, these estimates will be subject to some model mismatch. However, we demonstrated in our previous work that this approach still facilitates management of closed-loop variability when initially responding to setpoint errors, so long as integral tracking using the raw measurements is also employed (Ahmed et al., 2021a). The next section details MPC design with this integral tracking component.

3.2 Model Predictive Controller

A rate-based integral reference tracking MPC formulation was developed for feedback control. The formulation defines an extended system having a state vector

$$x_k^{\text{ext}} = \left[\Delta\hat{x}_k \;\; \hat{e}_k \;\; \hat{x}_{k-1} \;\; u_{k-1} \;\; z_{k-1}\right]^T \tag{7}$$

where $\Delta\hat{x}_k = \hat{x}_k - \hat{x}_{k-1}$ is the state estimate increment and $\hat{e}_k = \hat{y}_k - r_k$ is the estimated error relative to the phasing setpoint r_k. Both parameters use the output of the Kalman filter. The parameter z captures the discrete-time integrated error between raw stochastic phasing measurements and the setpoint, given by

$$z_k = z_{k-1} + T_s(y_{\text{phas},k} - r_k) \tag{8}$$

where $T_s = 0.1$ s is the timestep representing one engine cycle at 1200 rpm. For this extended system, the control input is the increment $\Delta u_k = u_k - u_{k-1}$. Then, the extended state prediction model is given by

$$x_{k+1}^{\text{ext}} = A^{\text{ext}}x_k^{\text{ext}} + B^{\text{ext}}\Delta u_k, \tag{9}$$

where

$$A^{\text{ext}} = \begin{bmatrix} A & 0 & 0 & 0 & 0 \\ CA & I_{n_e\times n_e} & 0 & 0 & 0 \\ I_{n_x\times n_x} & 0 & I_{n_x\times n_x} & 0 & 0 \\ 0 & 0 & 0 & I_{n_u\times n_u} & 0 \\ 0 & T_s & 0 & 0 & I_{n_z\times n_z} \end{bmatrix} \tag{10}$$

$$B^{\text{ext}} = \left[B \;\; CB \;\; 0 \;\; I_{n_u\times n_u} \;\; 0\right]^T. \tag{11}$$

Through the inclusion of $\hat{x}$, u, Δu, and z in the extended system model, integral setpoint tracking that enforces actuator range and rate constraints is possible. To tune the controller's actions toward these goals, a cost function for the extended system over a prediction horizon of N engine cycles is defined as

$$J_N = \sum_{k=0}^{N-1} (x_k^{\text{ext}})^T Q^{\text{ext}} x_k^{\text{ext}} + \Delta u_k^T R^{\text{ext}} \Delta u_k \tag{12}$$

where $Q^{\text{ext}} = \text{diag}(0, Q_e, 0, Q_u, Q_z)$ contains the penalties for the error estimate, actuator magnitude, and integrator state, respectively, and R^{ext} contains the penalties for actuation rate.

3.3 Quadratic Programming Formulation

To solve the MPC problem numerically, the cost function J_N is reduced to standard quadratic program (QP) form (Goodwin et al., 2004). From the discrete state transition formula, x_k^{ext} can be expressed as

$$x_k^{\text{ext}} = (A^{\text{ext}})^k x_0^{\text{ext}} + \sum_{i=0}^{k-1} (A^{\text{ext}})^{k-1-i} B^{\text{ext}} \Delta u_i, \tag{13}$$

where x_0^{ext} is the initial state vector.

Then, defining $U = [\Delta u_0 \ \Delta u_1 \ \dots \ \Delta u_{N-1}]^T$ as a vector of control vectors at each step in the horizon, and similarly $X = \left[x_1^{\text{ext}} \ x_2^{\text{ext}} \ \dots \ x_N^{\text{ext}}\right]^T$ as a vector of state vectors at each step in the horizon, X can be expressed as a linear function of U to provide the condensed form

$$X = SU + Mx_0^{\text{ext}} \tag{14}$$

where

$$\begin{aligned} S &= \begin{bmatrix} B^{\text{ext}} & 0 & \dots & 0 \\ A^{\text{ext}}B^{\text{ext}} & B^{\text{ext}} & \dots & 0 \\ \vdots & \vdots & \vdots & \\ (A^{\text{ext}})^{N-1}B^{\text{ext}} & (A^{\text{ext}})^{N-2} & \dots & B^{\text{ext}} \end{bmatrix} \\ M &= \left[A^{\text{ext}} \ (A^{\text{ext}})^2 \ \dots \ (A^{\text{ext}})^N\right]^T. \end{aligned} \tag{15}$$

Likewise, the control constraints and state constraints can be redefined as vectors of the respective constraint vectors at each step in the horizon such that

$$\begin{aligned} X_{\min} < X < X_{\max} \\ U_{\min} < U < U_{\max}. \end{aligned} \tag{16}$$

Combining Eq. 14 with Eq. 16 and augmenting the state and control constraints yields the constraints for the QP problem

$$GU \leq W + Tx_0, \tag{17}$$

where

$$G = \begin{bmatrix} S \\ -S \\ I \\ -I \end{bmatrix}, W = \begin{bmatrix} X_{\max} \\ -X_{\max} \\ U_{\max} \\ -U_{\min} \end{bmatrix}, T = \begin{bmatrix} -M \\ -M \\ 0 \\ 0 \end{bmatrix}. \tag{18}$$

Using Eq. 14, the cost function from Eq. 12 can be transformed into

$$\begin{aligned} J_N &= X^T\bar{Q}X + U\bar{R}U \\ &= U^T(S^T\bar{Q}S + \bar{R})U + 2(x_0^{\text{ext}})^TM^T\bar{Q}SU \\ &\quad + (x_0^{\text{ext}})^TM^T\bar{Q}Mx_0^{\text{ext}} + (x_0^{\text{ext}})^TQx_0^{\text{ext}} \\ &= U^THU + 2q^TU + c, \end{aligned} \tag{19}$$

where

$$\begin{aligned} \bar{Q} &= \begin{bmatrix} Q & \dots & 0 \\ \vdots & \ddots & \vdots \\ 0 & \dots & Q \end{bmatrix}, \bar{R} = \begin{bmatrix} R & \dots & 0 \\ \vdots & \ddots & \vdots \\ 0 & \dots & R \end{bmatrix} \\ H &= S^T\bar{Q}S + \bar{R} \\ q &= S^T\bar{Q}Mx_0^{\text{ext}} \\ c &= (x_0^{\text{ext}})^T(Q + M^T\bar{Q}M)x_0^{\text{ext}}. \end{aligned} \tag{20}$$

Finally, the MPC problem can be reduced to minimizing a quadratic function as follows:

$$\begin{aligned} \min_{U \in \mathbb{R}^{N \times n_u}} \ & J_N = U^THU + 2q^TU \\ \text{subject to: } & GU \leq W + Tx_0^{\text{ext}}. \end{aligned} \tag{21}$$

At each engine cycle, this QP problem is solved using the `quadprog` function in MATLAB to obtain the optimal N-step-forward rate-based control sequence Δu^*. The first element of this sequence is used to inform the control input to the engine for the next engine cycle: $u_k^* = u_{k-1} + [1 \ 0_{n_u \times N-1}]\,\Delta u^*$.

SOI was prioritized as the primary actuator because of its fast response time and significant control authority under many conditions. An IA device should only be used when needed, given its slow dynamics, parasitic power consumption, and fragility at high thermal loading. Thus, cost function parameters were tuned to ensure integral setpoint tracking in the presence of model mismatch and minimize IA usage unless SOI reaches its range limit. The tuned controller parameters are $N = 10$, $Q_e = 70$, $Q_u = \text{diag}(0, 0.01)$, $Q_z = 170$, and $R^{\text{ext}} = \text{diag}(0.01, 0.5)$.

4. CONTROLLER SIMULATION

The nonlinear virtual engine from Section 2.1 was controlled in simulation by the MPC scheme described in Section 3. Simulations were conducted on a computer with a 2.6 GHz Intel i7 processor. This section presents results investigating how MPC coordinates SOI and IA to track a desired combustion phasing trajectory. It also details how MPC autonomously adapts its tracking strategy as engine conditions and combustion phasing behavior evolve.

4.1 Injection Timing and Ignition Assist Coordination

Figure 4 presents simulation results of combustion phasing response to two step changes in desired combustion phasing. Stochastic combustion phasing output is shown along with a mean phasing approximation obtained from applying a Savitzky-Golay filter to the stochastic output. Initially, SOI sufficiently tracks the setpoint. The first step at engine cycle 100 advances desired phasing into a region where SOI alone lacks sufficient control authority. The controller predicts this limitation and activates IA to low power as an initial response. When tracking error persists, it ramps up IA power. Due to the additional control authority, combustion phasing shifts toward the setpoint, with a steady-state settling period of 68 cycles.

When the reference phasing retards at cycle 300, the controller recognizes that IA is no longer needed and ramps it down at 2 W/cycle while retarding SOI to track the new setpoint within 43 cycles. Throughout the simulation, CV in phasing remains less than 4% higher than the virtual engine's system or open-loop CV, indicating the feedback loop does not significantly amplify stochasticity. Thus the controller coordinates SOI with IA when needed to track desired combustion phasing, all while enforcing actuator range and rate constraints and managing closed-loop variability.

4.2 Impact of Horizon on Controller Performance

The step response simulation shown in Fig. 4 was repeated for different horizon lengths to understand how the MPC performance changes. Table 2 presents the controller's settling time t_{settle} when tracking a step command in desired phasing from 15 to 5 aTDC, the percent increase in closed-loop CV relative to the virtual engine's open-loop CV, and the simulation runtime per engine cycle.

As the horizon lengthens, the MPC scheme better coordinates actuators by more aggressively ramping up IA when SOI saturates. As a result, when tracking the step command the settling time decreases. Note that for $N \leq 4$, mean-value tracking is not achieved. The tradeoff observed here is that CV slightly increases as N increases, but

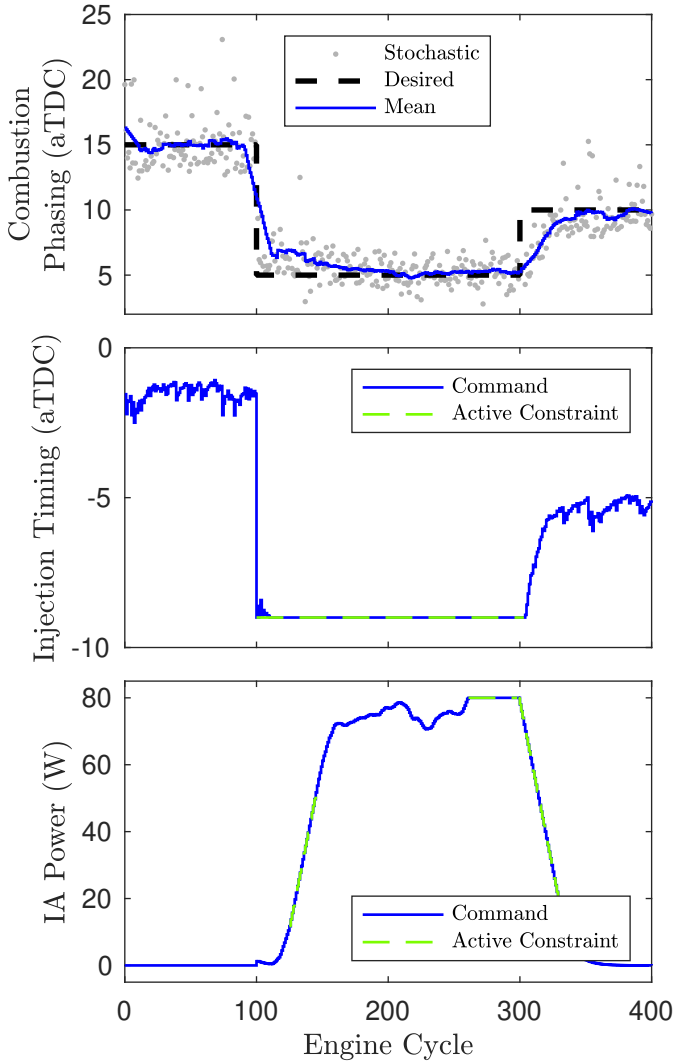

Fig. 4. The MPC scheme coordinates IA only when needed (cycles 100-300) to assist SOI in tracking desired combustion phasing. All actuator constraints are enforced (indicated in green).

ultimately the MPC maintains the amplification of CV to within 4%. As expected, when N increases the MPC takes longer per engine cycle to compute its next control action. Still, runtime results indicate that this MPC scheme is computationally tractable in real-time so long as an engine cycle is longer than 41 ms, meaning it is a feasible solution for engines running as fast as 2800 rpm. For the remainder of this work, simulations continued using $N = 10$.

Table 2. Step response performance as MPC prediction horizon N increases.

N(cyc)	t_{settle} (cyc)	% CV Increase	Runtime (ms/cyc)
4	N/A	1.6%	0.7
8	88	3.2%	3.1
10	68	3.5%	5.7
20	63	4.0%	41

4.3 Performance Over Evolving Engine Thermal State

The simulation presented in Figure 4 was conducted at a fixed engine thermal state, specified in the virtual engine model by an exhaust gas temperature value of $T_{\text{exh}} = 300$°C in accordance with experiments. However, as described in Section 2, during tests exhaust gas temperature increased by approximately 50°C as the engine warmed up from cold start. A successful MPC architecture for combustion phasing control should autonomously adapt its actuator command strategy over such a range of thermal conditions. Figure 5 presents four simulations at the different exhaust gas temperatures shown in Fig. 2, representing different engine thermal states. Each simulation uses the same reference combustion phasing trajectory, linear model for the feedback estimator and controller, and control parameters. The only difference, unbeknownst to the controller, is the exhaust temperature change in the nonlinear virtual engine system itself. The simulation results are overlayed on top of one another here for visual comparison, but physically they would represent repeating the same combustion phasing trajectory and MPC tracking exercise at four different times while the engine warms up from cold start. To avoid overcrowding the topmost panel of the figure, the mean-value of combustion phasing is plotted rather than the true stochastic output.

Just as in Figure 4, initially only SOI is needed to track the phasing setpoint. Because the steady-state combustion behavior shifts with thermal state, the integrator state of the MPC formulation drives it to identify a different "correct" SOI for each of the four simulations. In response to the first step in setpoint, the controller actuates IA differently depending on the thermal state. The colder the engine, the more aggressively the IA command ramps up toward its maximum power limit. For an intermediate thermal state, represented by $T_{\text{exh}} = 305$°C, the controller identifies a mid-range IA power of approximately 60 W because it is sufficient to track combustion phasing and facilitates conservation of the IA device. Once the engine's thermal state has warmed up to $T_{\text{exh}} = 340$°C, the combustion behavior has evolved such that IA is no longer needed at all, and the MPC scheme solely actuates SOI to track the phasing setpoint.

For quantitative perspective, the difference in combustion phasing behavior induced by this range of T_{exh} values is the equivalent of varying the controller's internal model, given in Eq. 4, by $|\Delta C| = [13\text{–}23\%\ 39\text{–}90\%]$. The second term here can be so high because during tests, the IA was observed to have limited impact on phasing when the engine had warmed up versus when still cold. These results demonstrate that the control strategy developed here can autonomously meet reference tracking and actuator constraint control objectives over a considerable range of engine behaviors without the need for retuning any internal model or control parameters.

5. CONCLUSION

As the automotive and aviation sectors look toward low-carbon and synthetic fuels, improved combustion control strategies for internal combustion engines are needed to support more diverse ignition behaviors. This work demonstrates for the first time that a model predictive controller can coordinate fuel injection timing and an ignition assisting heating element to control compression ignition combustion phasing on a cycle-to-cycle basis. Simulation

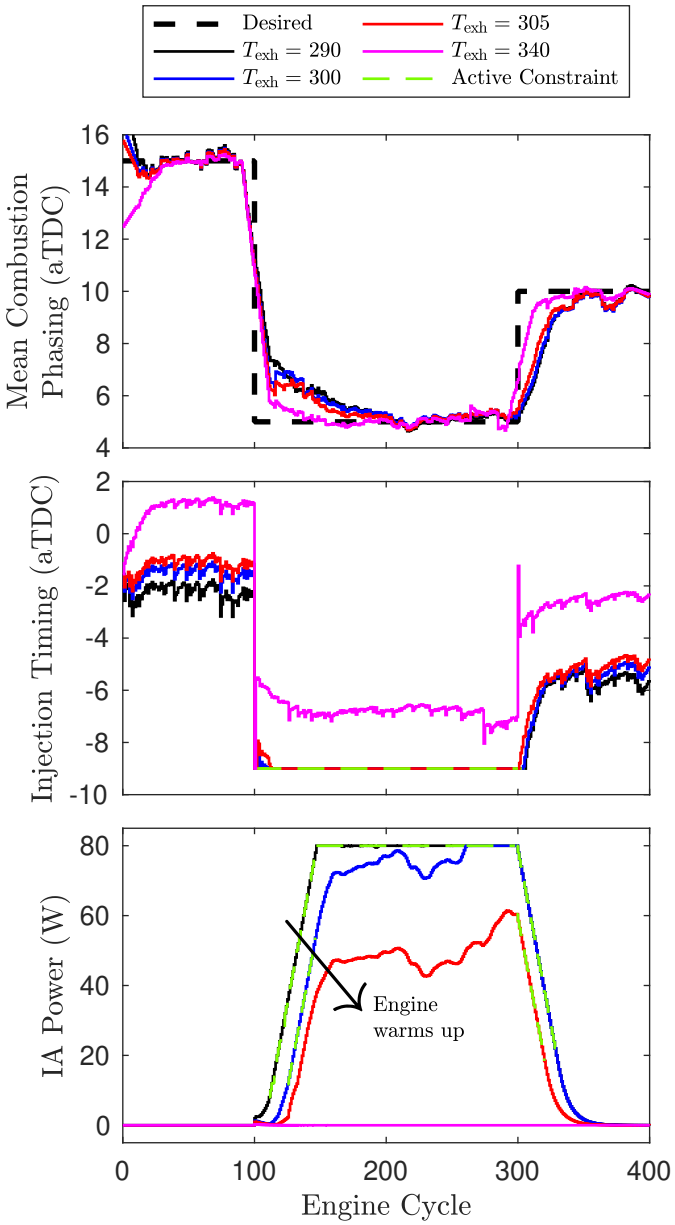

Fig. 5. Without retuning, the MPC autonomously adapts its actuator coordination strategy at four different engine thermal states while ensuring setpoint tracking.

results using a data-driven nonlinear virtual engine showed that the rate-based integral MPC formulation ensures reference combustion phasing tracking while conserving the ignition assist device by adhering to its strict range and rate constraints. Furthermore, the control scheme autonomously adapts its approach to coordinating the two actuators across a range of experimentally relevant combustion behaviors without the need for controller retuning. Future work may include experimentally validating this control scheme, as well as estimating combustion variability in real-time and augmenting the MPC formulation with a state that responds to excessive variability.

6. ACKNOWLEDGMENTS

Research was sponsored by the Army Research Laboratory under Cooperative Agreement Number W911NF-19-2-0208. The views and conclusions contained in this document are those of the authors and should not be interpreted as representing the official policies, either expressed or implied, of the Army Research Laboratory or the U.S. Government. The U.S. Government is authorized to reproduce and distribute reprints for Government purposes notwithstanding any copyright notation herein.

REFERENCES

Agarwal, A.K. (2007). Biofuels (alcohols and biodiesel) applications as fuels for internal combustion engines.

Ahmed, O., Middleton, R., Stefanopoulou, A., Kim, K., and Kweon, C.B. (2021a). Closed-loop diesel combustion control leveraging ignition assist. *IEEE Control Systems Letters*, 6, 1628–1633.

Ahmed, O., Middleton, R., Stefanopoulou, A., Kim, K., and Kweon, C. (2021b). Control-oriented model of the mean and dispersion of diesel combustion phasing with ignition assist. *Proceedings of the ASME 2021 Internal Combustion Engine Division Fall Technical Conference*.

Bergmann, D., Harder, K., Niemeyer, J., and Graichen, K. (2021). Nonlinear MPC of a Heavy-Duty Diesel Engine With Learning Gaussian Process Regression. *IEEE Transactions on Control Systems Technology*, 30(1), 113–129.

Duraiarasan, S., Stefanopoulou, A., Middleton, R., Salehi, R., Mahesh, S., and Allain, M. (2021). Diesel Engine Transient NOx and Airpath Control using Rate-based Model Predictive Controller. *IFAC-PapersOnLine*, 54(10), 21–26.

Goodwin, G., Seron, M.M., de Dona, J.A., and de Dona, J.A. (2004). Constrained control and estimation, an optimisation approach. *Communications and Control Engineering Ser.*

Hillion, M., Bulhbuck, H., Chauvin, J., and Petit, N. (2009). Combustion control of diesel engines using injection timing. *SAE World Congress and Exhibition*, SAE 2009-01-0367.

Lawler, B., Lacey, J., Guralp, O., Najt, P., and Filipi, Z. (2018). HCCI combustion with an actively controlled glow plug: The effects on heat release, thermal stratification, efficiency, and emissions. *Applied Energy*, 211, 809–819.

Motily, A.H., Ryu, J.I., Kim, K., Kim, K., Kweon, C.B.M., and Lee, T. (2021). High-pressure fuel spray ignition behavior with hot surface interaction. volume 38, 6763–6772. Elsevier Ltd.

Oprea, C., Wong, F., Sharif, H.K., Troczynski, T., Blair, C., and Welch, A. (2012). Degradation of Silicon Nitride Glow Plugs in Various Environments Part 3: NGDI Engine.

Willems, F. (2018). Is cylinder pressure-based control required to meet future HD legislation? *5th IFAC Conference on Engine and Powertrain Control, Simulation, and Modeling*, 51(31), 111–118.

Yilmaz, N. and Atmanli, A. (2017). Sustainable alternative fuels in aviation. *Energy*, 140, 1378–1386.

Zhou, T., Yao, C., Hu, Y., Yang, F., Wang, J., and Ouyang, M. (2016). Research on performance and temperature control of glow plugs for PPCI low load assist. *8th IFAC Symposium on Advances in Automotive Control*, 49(11), 223–230.